

OPTIMIZATION OF THE PARAMETERS OF A STORAGE RING FOR A HIGH POWER  
XUV FREE ELECTRON LASER\*

A. Jackson, J. Bisognano, S. Chattopadhyay, M. Cornacchia, A. Garren,  
K. Halbach, K. J. Kim, H. Lancaster, J. Peterson, M. S. Zisman

Lawrence Berkeley Laboratory  
University of California  
Berkeley, California 94720

C. Pellegrini, G. Vignola  
Brookhaven National Laboratory  
Upton, L.I., New York 11973

---

\* This work was supported by the Director, Office of Energy Research, Office of High Energy and Nuclear Physics, High Energy Physics Division, U.S. Dept. of Energy, under Contract No. DE-AC03-76SF00098 and, in part, under Brookhaven National Laboratory DOE Contract No. DE-AC02-76CH00016.

A. Jackson, J. Bisognano, S. Chattopadhyay, M. Cornacchia, A. Garren, K. Halbach,  
K.J. Kim, H. Lancaster, J. Peterson, M. S. Zisman

Lawrence Berkeley Laboratory  
#1 Cyclotron Rd. MS 47-112  
Berkeley, California 94720

C. Pellegrini, G. Vignola

Brookhaven National Laboratory  
Upton, L.I., New York 11973

### Abstract

In this paper we describe the operation of an XUV high gain FEL operating within a bypass of an electron storage ring, and discuss the implications on storage ring optimization imposed by FEL requirements. It transpires that, in the parameter regime of interest, collective effects within the beam play an important role. For example, intrabeam scattering dilutes the transverse emittance of the beam and the microwave instability increases the momentum spread. Both phenomena reduce the effectiveness of the FEL. A computer code, ZAP, has been written which, for a given lattice design, takes all such effects into consideration and produces a figure of merit for FEL operation for that machine. We show the results of ZAP for several storage ring designs, all optimized for FEL operation, and present a design example of a facility capable of producing coherent radiation at 400 Å with tens of megawatts of peak power.

### 1. Introduction

There has recently been remarkable progress in demonstrating the generation of coherent radiation through Free Electron Laser (FEL) interaction in the infrared and microwave region (Ref. 1). With electron beams of suitable quality, the technique could be extended to wavelengths shorter than 1000 Å.

With present day technology, there are two promising approaches to the vacuum ultraviolet (XUV) FEL. One is based on cavity formation by end mirrors (Refs. 2 and 3), the other through the development of high gain in a single pass device. The former "FEL oscillator" is currently restricted to longer wavelengths because high reflectivity mirrors (although rapidly evolving through multilayer technology) are not yet available (Ref. 2). In the second approach, which we call the High Gain FEL, the interaction between the electron beam and the undulator occurs in a single pass, and no mirrors are required.

The most promising source of electrons with the characteristics required for FEL operation is an electron storage ring. The mode of operation is to deflect the circulating electron bunch into a special bypass containing the FEL undulator, as shown schematically in Figure 1. The beam, which is severely disrupted in the FEL interaction is then reinjected into the storage ring, where its equilibrium characteristics are restored through the process of radiation damping. After one damping time (50-100 ms), the beam is ready to be switched back into the FEL bypass and the process is repeated. References 4 and 5 give a more detailed description of FEL bypass operation.

In this paper we show how the evolution of the optical pulse in the FEL is determined by certain characteristics of the electron pulse, in particular, the charge density and momentum spread. We show how these requirements lead to conflicting demands on the storage ring design, and how these conflicts have been assessed in a systematic fashion through the development of a new computer code, ZAP.

This novel, systematic approach has been used to choose between candidate storage ring lattices, all of which were optimized for high gain FEL operation. Based on our study we present a design example that is capable of producing coherent radiation at 400 Å with tens of megawatts peak power.

## 2. FEL Issues

### FEL Gain, Power, Saturation Length

An electron beam of energy  $\gamma m_e c^2$  traveling through a magnetic undulator of period  $\lambda_u$  can interchange energy with a transverse laser field of wavelength  $\lambda$  propagating in the same direction (Refs. 6 and 7). The interaction becomes resonant when the following condition is satisfied:

$$\lambda = \frac{(1 + K^2/2)}{2\gamma^2} \lambda_u \quad (2.1)$$

where  $K$  is the deflection parameter, characteristic of the undulator, given by

$$K = \frac{e \lambda_u B}{2\pi m_e c} = 0.934 \lambda_{u[\text{cm}]} B \quad [\text{Tesla}] \quad (2.2)$$

An important quantity, which determines the FEL characteristics in the one-dimensional theory, is the dimensionless parameter  $\rho$ , given by (Ref. 8)

$$\rho = \left( \frac{K^2 [JJ] \tau_e n_b \lambda_u^2}{32\pi\gamma^3} \right)^{1/3} \quad (2.3)$$

where

$$[JJ] = [J_0(\xi) - J_1(\xi)]^2 \quad \text{with } \xi = \frac{K^2}{4(1 + K^2/2)} \quad (2.4)$$

The  $J_0$  and  $J_1$  are ordinary Bessel functions of order zero and one, respectively. As will emerge in the course of this paper, for the parameters of interest to us,  $\rho$  is typically of the order of  $10^{-3}$ .

The characteristics of the power growth of the laser wave, as obtained from the one-dimensional theory, fall into three distinct regimes: the small-signal regime, the exponential-growth regime and the saturation regime. Near the entrance of the undulator, where the small-signal theory applies, the gain  $G$  (defined as the ratio of the laser power at two points separated by a distance  $z$  along the undulator axis) is given by

$$G = 536 (\rho z / \lambda_u)^3 \quad (2.5)$$

Farther along the undulator, the laser power  $P$  grows exponentially (Refs. 9 to 14) with distance, from the initial power  $P_0$  at a rate proportional to:

$$P = \frac{P_0 e^{gz}}{9} \quad (2.6)$$

where

$$g = 4\pi\sqrt{3}(\rho/\lambda_u) \quad (2.7)$$

The corresponding e-folding length for the growth of the radiation power in the exponential growth regime is

$$l_e = g^{-1} = \frac{1}{4\pi\sqrt{3}} \frac{\lambda_u}{\rho} \quad (2.8)$$

Eventually, the electrons are captured in the ponderomotive potential well and the growth of radiation power stops. The laser saturates at a distance  $z = z_{\text{sat}}$  with a characteristic saturated peak power  $P_{\text{sat}}$ . The saturation length and the peak power are given approximately by (Ref. 8)

$$z_{\text{sat}} \approx (\lambda_u / \rho) \quad (2.9)$$

$$P_{\text{sat}} \approx \rho P_{\text{beam}} \quad (2.10)$$

where  $P_{\text{beam}} = \hat{I}E/e$  is the peak power in the electron beam. The optimum choice for the number of undulator periods  $N$  is given by

$$N = (z_{\text{sat}} / \lambda_u) \approx (1/\rho) \quad (2.11)$$

This choice for the number of undulator periods maximizes the laser power in the shortest possible undulator length.

Taking the typical values of  $\hat{I} = 200$  A,  $E = 750$  MeV and  $\rho = 1 \times 10^{-3}$  considered in this paper, one obtains from Eqn. (2.10) a peak laser power of 150 MW. Assuming a beam pulse length of 100 psec and a repetition time (equal to the typical longitudinal damping time of the storage ring) of 50 msec, we obtain an average power of 0.3 watts.

A coherent source of radiation of such high intensity, both in peak and average power, would certainly pioneer novel scientific applications.

#### Relationships Between Laser Power and Electron Beam Parameters

We have seen that the FEL parameter  $\rho$  determines the peak power that can be obtained from the laser. In what follows, we try to relate this parameter to the electron beam and storage ring characteristics.

The volume density of the bunched electron beam is

$$n_b = \frac{\hat{I}}{ec2\pi\sigma_x\sigma_y} \quad (2.12)$$

The beam size  $\sigma_{x,y}$  can be expressed in terms of the emittances  $\epsilon_{x,y}$  and the amplitude functions  $\beta_{x,y}$ :

$$\sigma_{x,y} = \sqrt{\epsilon_{x,y} \beta_{x,y}} \quad (2.13)$$

The alternating field of an undulator provides an effective focussing force. For a planar undulator, the focussing is in the vertical direction, with an effective  $\beta$ -function given by (Ref. 15)

$$\beta_y = \frac{\lambda_u \Upsilon}{\sqrt{2} K \pi} \quad (2.14)$$

Horizontal focussing can also be provided by tilting or by shaping the pole surfaces of the undulator (Ref. 16). In either case, the focussing strength in the vertical plane is thereby reduced. For the purpose of conceptual simplicity, we assume a focussing force of the same magnitude in both directions:

$$\beta_x = \beta_y = \frac{\lambda_u \Upsilon}{K \pi} \quad (2.15)$$

By combining Eqns. (2.1), (2.12), (2.13), and (2.15), the FEL parameter given in Eqn. (2.3) can be rewritten:

$$\rho^3 = \frac{1}{16\pi} \frac{\Upsilon e}{ec} \frac{K^3 [JJ]}{2(1+K^2/2)} \frac{\lambda}{\Upsilon^2 \sqrt{\epsilon_x \epsilon_y}} \hat{I} \quad (2.16)$$

The above results apply only to the one-dimensional theory with zero energy spread. If a finite energy spread is taken into account, the growth rate and the saturation power are modified as follows (Ref. 17):

$$\begin{aligned} g &\rightarrow g' = f(\sigma_p, \rho)g \\ P_{\text{sat}} &\rightarrow P'_{\text{sat}} = h(\sigma_p, \rho) P_{\text{sat}} \end{aligned} \quad (2.17)$$

The  $f(\sigma_p, \rho)$  and  $h(\sigma_p, \rho)$  are functions of the electron relative energy spread,  $\sigma_p = (\Delta p/p)_{\text{rms}}$ , and  $\rho$ , and describe form factors that, in general, decrease with increasing values of  $(\sigma_p/\rho)$ . If  $\sigma_p$  is non-zero, the FEL performance is significantly reduced unless the following condition is satisfied (Ref. 18):

$$\sigma_p \leq 1/N - \rho \quad (2.18)$$

If the momentum spread of the electron beam is large and the inequality in Eqn.(2.18) is violated, both functions  $f$  and  $g$  can become considerably less than unity, thus degrading the FEL performance. The function  $f(\sigma_p, \rho)$  can be obtained by solving a dispersion relation, which becomes a cubic equation for a Lorentzian or a rectangular longitudinal momentum distribution. For a Lorentzian distribution, the value of  $f(\sigma_p, \rho)$  is 1 when  $\sigma_p/\rho = 0$  and 0.36 when  $\sigma_p/\rho = 1$ .

In addition to the natural energy spread, the beam emittance contributes an effective energy spread (Ref. 5) that is subject to a condition similar to Eqn. (2.18). Making use of Eqn. (2.15) and under the assumption that the transverse charge distributions are Gaussian, the effective energy spread can be written:

$$(\sigma_p)_{\text{eff}} = \frac{\sqrt{(c_x^2 + 5c_y^2)} \pi}{2\sqrt{2} \gamma \lambda} \quad (2.19)$$

For all the cases considered in this paper, the effective energy spread is not negligible, but is usually smaller than the natural  $\sigma_p$ .

In determining a "Figure of merit" for a given storage ring by which it may be compared with others, we attempt to achieve the maximum peak power output in the shortest undulator length for a given output wavelength. We see from equations (2.6) and (2.8) that this requires maximizing the gain parameter,  $\rho$ . In terms of the storage ring design, we see that maximizing  $\rho$  involves maximizing the value of  $\bar{I}/(\gamma^2 \sqrt{c_x c_y})$ , i.e., maximizing the current density. In the next section we discuss the problems of achieving high density electron bunches in a storage ring.

### 3. Problems in Achieving High Density Electron Bunches and Their Implications for Storage Ring Design

In this section we review the collective effects that limit the electron density achievable in a storage ring and show how they demand conflicting requirements from the ring design.

The interaction of the beam with its environment produces electromagnetic fields which react back on the beam. This feedback mechanism causes a variety of coherent instabilities to develop that either cause the momentum spread to increase or limit the maximum achievable current. Either effect is deleterious to FEL performance.

For the FEL rings we have considered, the longitudinal microwave instability presents the most severe limitation. Here the threshold peak current is given by (Ref. 19):

$$\bar{I}_L = \frac{2\pi\alpha\sigma_p^2(E/e)F_L}{(Z_L/n)_{\text{eff}}} \quad (3.1)$$

where  $F_L$  is the longitudinal form factor ( $\approx 1$ ) and  $(Z_L/n)$  is the effective longitudinal impedance, which is the average of the full frequency dependent impedance over the bunch mode spectrum.

Already we can see conflicting requirements. From equation (2.18) we wish to keep  $\sigma_p$  small, which from equation (3.1) lowers the peak current achievable. This could be offset by designing a lattice with a large momentum compaction factor,  $\alpha$ . However, increasing  $\alpha$  demands a larger rf voltage to maintain the momentum acceptance of the storage ring, which in general will result in more rf cavities and thereby more longitudinal impedance.

This aspect of parameter optimization is further exacerbated by the requirements of another effect, intrabeam scattering. In this process electrons within the bunch Coulomb scatter off each other transferring energy predominantly from transverse into longitudinal motion. When such a scatter occurs in a dispersive region of the lattice, a radial betatron oscillation is excited. The net result is that the beam grows both radially and longitudinally, thereby increasing the emittance and diluting the bunch density.

Quantitatively, the treatment of intrabeam scattering is quite complicated (Ref. 20). However, for the type of lattices under consideration, an approximate expression for the radial diffusion rate was found to be:

$$\frac{1}{\tau_x} = \frac{c \bar{I}}{c_x^2} \left\langle \frac{\sqrt{H}}{\sigma_p \gamma^3 \sqrt{\beta_y}} \right\rangle \quad (3.2a)$$

where H is given by: 
$$H = \gamma_x \eta^2 + 2\alpha_x \eta \eta' + \beta_x \eta'^2 \quad (3.2b)$$

with  $\alpha_x$ ,  $\beta_x$  and  $\gamma_x$  being the lattice Twiss parameters,  $\eta$  the dispersion function and  $\eta'$  its derivative.

It is immediately seen that all the requirements for the high gain FEL tend to increase the diffusion rate. Moreover, buried in H is a requirement to reduce the dispersion in the lattice and so reduce  $\alpha$ , in direct conflict with the requirement on  $\alpha$  from the longitudinal microwave instability.

Large angle Coulomb scattering results in a longitudinal (momentum) excursion which can kick the electron out of the momentum acceptance of the storage ring. This well known phenomenon known as the Touschek effect leads to a reduced lifetime of the stored electron beam. The Touschek lifetime is proportional to the cube of the energy ( $\gamma^3$ ), the square of the momentum acceptance, and inversely to the beam density. Thus, increasing the Touschek lifetime moves in the direction of reducing the FEL gain,  $\rho$ .

By now it should be apparent that there is little chance of finding a prescription by which storage ring parameters can be found to simultaneously satisfy the various constraints. What is required is a way in which to judge the suitability of a given lattice for a given application, in this case, the XUV-FEL. To this end we have begun the development of a new computer code called ZAP.

In broad outline, the program works as follows. As primary inputs, ZAP utilizes the parameters of a lattice (betatron functions, dispersion, momentum compaction, natural emittance, radiation damping time) along with the relevant "physics" needs (e.g., the FEL requirement for small momentum spread). The code then calculates, as a function of the rms bunch length, the required rf voltage and the corresponding bucket height. Impedance estimates are made and, based on these, calculations of the longitudinal and transverse threshold currents. From the lower of these threshold current values and the radiation damping time, ZAP calculates the intrabeam scattering (IBS) rates and iterates to find the equilibrium transverse and longitudinal emittances (where the IBS and the quantum excitation are balanced by the radiation damping). Finally, the equilibrium emittance values and a selected momentum acceptance are used to obtain the Touschek lifetime of the ring. Other options of the code include calculation of the primary FEL parameters, gas scattering lifetime, and estimates of multibunch instability growth rates and frequency shifts.

Thus, from the earliest stages of a lattice design, ZAP can be used to indicate whether or not the design is worth pursuing and, if so, in which directions improvements could be made. Details of the way in which the code works can be found in Ref. 22.

A good example of the use of ZAP is the determination of parameter variation with the allowed momentum spread of the beam,  $\sigma_p$ . In terms of the peak current limitation, one of the ways of gaining (as can be seen<sup>D</sup> in Eqn. (3.1)) is to increase the allowable momentum spread of the beam. For low values of  $\sigma_p$ , we expect the peak current to increase as  $\sigma_p^2$ . At larger values of  $\sigma_p$  this increase flattens out, because the impedance becomes rf dominated, and thus the impedance is also increasing quadratically with  $\sigma_p$ . (In this latter regime the longitudinal threshold is no longer dominant anyway.) Below  $\sigma_p$  of about 0.005, the peak current limitation arises from the longitudinal threshold, whereas above this value the transverse threshold would dominate. Obviously the peak current performance improves with increasing momentum spread. Unfortunately, the gain of an FEL degrades rapidly if  $\sigma_p$  is greater than the  $\rho$  parameter. This degradation of FEL performance with increasing momentum spread is illustrated in Fig. 2, which shows the increase in e-folding length ( $l_{eff}$ ) and decrease in gain parameter ( $\rho_{eff}$ ) compared with their zero-energy-spread values ( $l_{e,\rho}$ ). For the designs considered here, we conclude that the value of  $\sigma_p$  that can be achieved in the storage ring (as a compromise between storage ring and FEL performance) is about 0.002.

#### 4. The Coherent XUV Facility (CXF)

For the parametric studies of the lattices considered for the CXF, some common assumption were made. For example, impedance estimates for the ring include the "SPEAR roll-off" when bunch lengths are shorter than the average beam pipe radius. Included in the impedance estimate is the contribution from the rf cavities. For the rings to be discussed in this paper, we standardized on the 500 MHz rf cavity used in PETRA. The required number of rf cells is estimated (assuming a peak rf voltage of 500 kV/cell) based on the voltage needed to maintain a beam of the chosen momentum spread and bunch length within the linear part of the rf acceptance. (This estimate leads to a minimum rf requirement, which is preferred for both economic and impedance reasons.) Based on measurements of the PETRA cavities (Ref. 21), we have assumed a contribution to the longitudinal broadband impedance of  $3.66/R$  ohms/cell and a transverse contribution per cell of 4,000 ohms/m.

Five different lattices of three types were investigated for the CXF. Details of the lattices and a discussion of how their parameters evolved can be found in Ref. 22.

In each case, the viability of the lattice (tunability, chromatic behaviour, dynamic aperture, etc.) has been confirmed, and the parameters optimized to give the best performance in terms of a CXF. A summary of each lattice, and the results of the analysis using ZAP, are presented in Tables 1 and 2, respectively.

Table 1. Summary of Lattice Parameters

Lattice Parameters	SF180W	SF130W	SF130	CF155	CF144	Units
$v_x$	6.61	6.65	6.37	7.35	7.85	
$v_y$	6.64	4.64	2.12	4.35	4.35	
$\alpha \times 10^3$	14.4	5.77	5.90	5.62	4.92	
$\eta_{max}$	2.67	1.43	1.43	0.80	0.70	m
$U_0$	39.6	46.3	10.3	7.0	8.0	keV/turn
$\tau_c \times 10^3$	11.4	7.0	31.9	68.6	52.3	s
$K_F \hat{z}$ (sextupole)	0.79	1.05	1.09	3.01	4.94	$m^{-2}$
$K_D \hat{z}$ (strength)	-0.99	-2.88	-2.24	-3.2	-4.60	$m^{-2}$
$\beta_x$ (max)	36.4	24.3	26.2	16.6	16.7	m
$\beta_y$ (max)	31.9	24.2	33.5	28.8	29.3	m
$V_0$	4.7	1.4	1.4	1.6	1.3	MV
$c_{ox} \times 10^3$	3.25	6.85	21.5	5.0	4.6	m-rad

Table 2. Parameters Predicted by ZAP

Lattice Parameters	$c_x/c_y$	SF180W	SF130W	SF130	CF155	CF144	Units
$\hat{c}_x \times 10^3$	10:1	10.2	7.4	24.8	12.9	10.1	m-rad
$\hat{I}$		376	123	230	214	199	A
$\sigma_z$		0.0125	0.0125	0.0125	0.0125	0.0125	m
$\tau_T$	10:1	1.0	2.4	3.7	2.0	1.4	h
$\frac{\hat{I}}{\sqrt{c_x c_y}} \times 10^{-10}$	{ 1:1 { 10:1 { 100:1	9.4 11.6 19.2	3.3 5.3 11.8	1.8 2.9 7.2	4.2 5.2 8.7	5.0 6.2 10.5	A $m^{-1}$
$\rho \times 10^3$	10:1	1.6	1.3	1.0	1.3	1.3	

Solely in terms of the FEL gain parameter,  $\rho$ , the lattice SF180W (a Chasman-Green structure with high field wiggler insertions to improve the synchrotron damping rates) has the best figure of merit. However, it has not been chosen as the preferred solution amongst other lattice options. It is perhaps worthwhile to summarize here what seemed to us to be the drawbacks of this lattice.

- The operation of a storage ring with a relatively large proportion of its circumference occupied by high field wiggler magnets like SF180W may present problems, or at least introduces an element of uncertainty in the beam dynamics aspects of the storage ring. The non-linear effects of high field wigglers on the long term stability of the beam are not yet known, and more theoretical and experimental work is needed.
- Free space for conventional undulators has been reserved in the lattice. It is beyond the scope of this paper to discuss the detailed aspects of the machine operating in the more conventional undulator mode. These undulators would probably operate at different beam energies from the FEL. Different optics solutions would be needed for the two modes of operation (FEL operation at low energy and conventional undulator operation at the peak energy of 1.3 GeV).
- The large energy acceptance (3%) needed for an acceptable Touschek lifetime requires a powerful rf system (4.7 MV peak voltage at 750 MeV compared with 1.3 MV for lattice CF144, for example).
- Large dynamic and physical apertures are required to accept an electron that experiences a momentum change of 3% due to Coulomb scattering within the achromat, where the peak dispersion is 2.7 m.
- It was found that the chromatic properties of this lattice are very sensitive to the exact location of the chromaticity sextupoles.

The lattices designated "CF" are Vignola-type combined function lattices (Ref. 23), which give emittance values comparable to those of the separated function lattices having wigglers. Moreover, they have the operational simplicity that a lattice with wigglers does not have, e.g., easy energy variability and excellent chromatic properties. Although there is some penalty in FEL performance, the simplicity and relative cost-effectiveness of this type of lattice make it appear a good candidate for further study. For these reasons, we have adopted the lattice CF144 as our choice for presentation as the design example for the CXF.

A detailed discussion of lattice CF144 can be found in Ref. 22, together with a description of some of the necessary facility subsystems (injector, rf, bypass, and undulator). Here we present for completeness a layout drawing of the facility, Figure 3, and the lattice functions through one of the (six) unit cells, Figure 4.

With the parameters outlined in Table 2, i.e.,  $\bar{I} = 199$  A at 750 MeV,  $\sigma_p = 2 \times 10^{-3}$  and  $\rho = 1.3 \times 10^{-3}$ , we obtain an effective gain parameter of  $\rho_{eff} = 0.2 \times 10^{-3}$  (see Figure 2), which gives a peak power in the optical pulse of  $\sim 30$  MW.

The FEL bypass system which complements CF144 has also been designed. The layout of the extraction elements leading to the FEL undulator is shown in Figure 5, and the matched optical functions along this section of the bypass are given in Figure 6. Reinjection into the storage ring from the bypass is a mirror image of the extraction side.

Finally, let us consider the FEL undulator itself. It is seen from Eqn. (2.16) that a high value of the deflection parameter  $K$  is desirable. As  $K$  ranges from 0 to infinity in Eqn. (2.4), the argument  $\xi$  of the Bessel functions in  $[JJ]$  ranges only from 0 to 0.5; thus,  $[JJ]$  becomes constant as  $K$  increases. For large  $K$ ,  $\rho^3$  is simply proportional to  $K$ . For fixed  $\lambda$  and  $\gamma$ , a higher  $K$  demands a smaller undulator period  $\lambda_u$  in order to satisfy the resonant condition (see Eqn. (2.1)). Note that this is consistent with the demand for a smaller saturation length ( $z_{sat} = \lambda_u/\rho$ ).

From Eqn. (2.2) we see that if one wants a smaller undulator period without reducing  $K$ , the undulator field  $B$  must increase. This requires reducing the undulator gap. We use the following approximate empirical relation for the field of a hybrid undulator having a steel-permanent-magnet (samarium-cobalt, Ref. 24) design:

$$B[\text{tesla}] = 3.34 \exp \left\{ -\frac{d}{\lambda_u} \left[ 5.47 - 1.8 \frac{d}{\lambda_u} \right] \right\} \quad (4.1)$$

where  $d$  is the undulator gap.

In practice, the deflection parameter  $K$  cannot be increased too much, or else the effective energy spread in Eqn. (2.19) becomes significant and degrades the FEL performance. Even with this constraint, the undulator gap is still small enough to significantly disrupt the beam, thus requiring a bypass for the FEL (Ref. 22). The undulator parameters of interest in our design are summarized in Table 3.

Table 3 Undulator Parameters

Photon wavelength (Å)	400		1000	
	500	750	500	750
Electron energy (MeV)	1.85	2.29	2.36	2.91
Magnet period (cm)	2.50	3.61	3.77	5.26
K	1.45	1.67	1.71	1.93
Peak Magnetic Field (T)	2.31	2.97	1.95	2.59
$\beta_x = \beta_y$ (m)				

Undulator gap : 0.3 cm

### 5. Summary and Conclusions

We have shown that in a single pass, high gain FEL driven by an electron storage ring, the ultimate performance of the FEL is intrinsically tied to the electron beam parameters. It is demonstrated that high charge densities are required and that, in such a regime, collective effects dominate the equilibrium behaviour of the stored beam. In order to identify the parameter dependence, we have written a new computer program, called ZAP, which has been used to select and optimize a particular storage ring lattice structure for use in an XUV coherent radiation facility. The viability of such a facility has been confirmed and we predict an output power of ~30 MW peak, at a repetition rate of ~20 Hz.

### Acknowledgment

This work was supported by the Director, Office of Energy Research, Office of High Energy and Nuclear Physics, High Energy Physics Division, U.S. Dept. of Energy, under Contract No. DE-AC03-76SF00098.

### References

1. See the contributed papers to the Castelgandolfo 1984 FEL Conference, Nucl. Inst. and Methods in Physics Research, to be published (1985).
2. D.T. Attwood et al., in Free Electron Generation of Extreme Ultraviolet Coherent Radiation, J.M.J. Madey and C. Pellegrini, eds., Amer. Inst. Phys., New York, 1984, (Conf. Proc. No. 118), p.294.
3. C. Pellegrini, Nucl. Inst. Meth., 177, 227 (1980).
4. An experiment on the High Gain FEL in the microwave range was carried out by a Lawrence Berkeley Laboratory/Lawrence Livermore National Laboratory Group. W.B. Colson and A.M. Sessler, 'Free Electron Lasers', LBL-18905 (January 1985), submitted to Annual Reviews of Nuclear and Particle Science. T.J. Orzechowski, et al., UCRL-91559 (September 1984), submitted to Phys. Rev. Lett.
5. J. Murphy and C. Pellegrini, Intl. Quant. Elec. Conf., Paper WQQ2, San Diego, CA (June 1984).
6. For a review, see for example, W.B. Colson, Physics of Quantum Electronics, 8 (FEL Generation of Coherent Radiation, S.F. Jacobs et al. eds., Addison-Wesley, 1982), p. 457.
7. J. M. J. Madey, J. Appl. Phys., 42, 1906 (1971); and J. M. J. Madey, M. A. Schwettman, W. M. Fairbank, IEEE Trans. Nucl. Sci., NS-20, 980 (1973).
8. B. Bonifacio, C. Pellegrini and N. Narducci, in Free Electron Generation of Extreme Ultraviolet Coherent Radiation, J.M.J. Madey and C. Pellegrini, eds. (Amer. Inst. Phys., New York, 1984), p. 236.
9. N.M. Kroll and W.A. McMullin, Phys. Rev., A17, 300 (1978).
10. A. Gover and Z. Livni, Opt. Comm., 26, 375 (1978).
11. I.B. Bernstein and J.L. Hirshfeld, Phys. Rev., A20, 1661 (1979).

12. P. Sprangle, C.M. Tang and W.M. Manheimer, Phys. Rev., A21, 302 (1980).
13. C.C. Shih and A. Yariv, IEEE J. Quant. Electron., QE-17, 1387 (1981).
14. G. Dattoli, A. Marino, A. Renieri and F. Romanelli, IEEE J. Quant. Electron., QE-17, 1371 (1981).
15. Calculations by, for instance, K. Halbach. See also Ref. 17.
16. E.T. Scharlemann, Lawrence Livermore National Laboratory, ELF Note 105 (July 1984).
17. K. J. Kim and J. M. Peterson, "Storage Ring Parameters for High Gain FEL," Lawrence Berkeley Laboratory, Paper presented at the 1985 Particle Accelerator Conference, Vancouver, BC, Canada, May 13-16, 1985.
18. J. Murphy, C. Pellegrini, B. Bonifacio, Optics Communications, 53, 197 (1985).
19. For a review, see, for instance, C. Pellegrini, Brookhaven National Laboratory Report 51538 (April 1982), and J.L. Laclare; Xith Intl. Conf. on High Energy Accelerators, Geneva (1980), p.526.
20. J.D. Bjorken and S.E. Mtingwa, Particle Accelerators, 13, 115 (1983).
21. T. Weiland, DESY Report 83-005, February, 1983.
22. J. Bisognano, et al., "Feasibility Study of a Storage Ring for a High Power XUV Free Electron Laser," (LBL-19771, June, 1985), to be published in Particle Accelerators.
23. G. Vignola, "Preliminary Design of a Dedicated 6 GeV Synchrotron Radiation Storage Ring", Submitted to Nucl. Inst. Meth.
24. K. Halbach, Journal de Physique Colloque, C1, 44, 211 (1983).

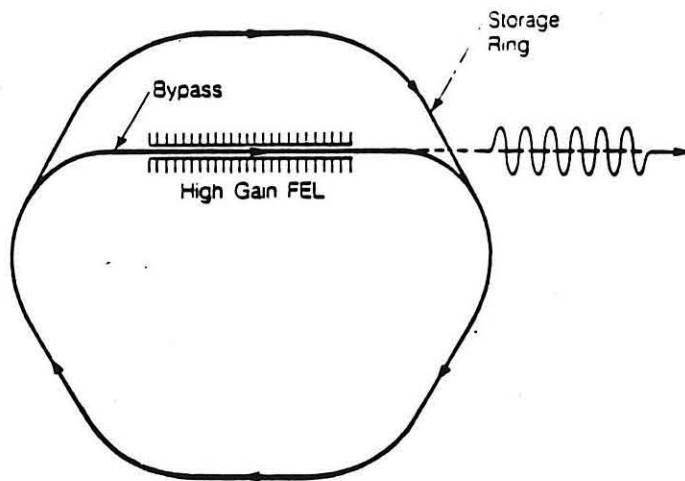


Fig. 1 Schematic drawing of a storage ring with a bypass containing a high gain FEL.

XBL 854-10171

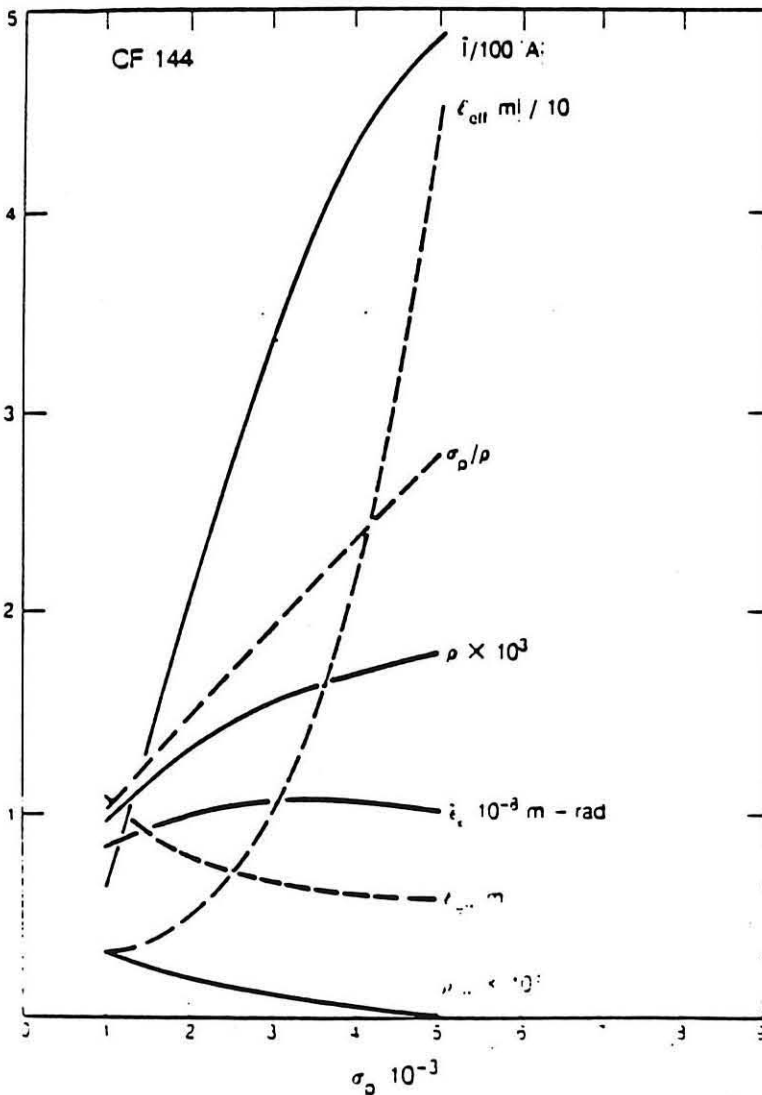
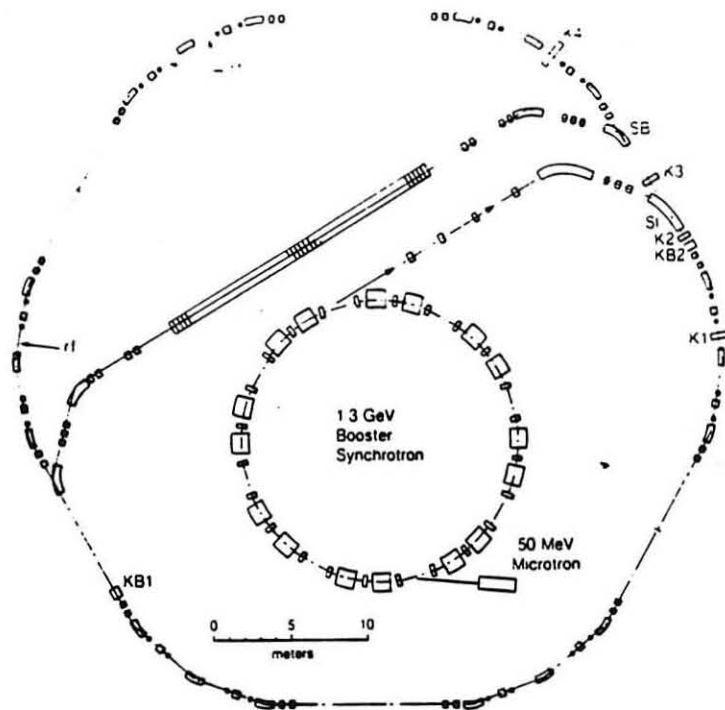


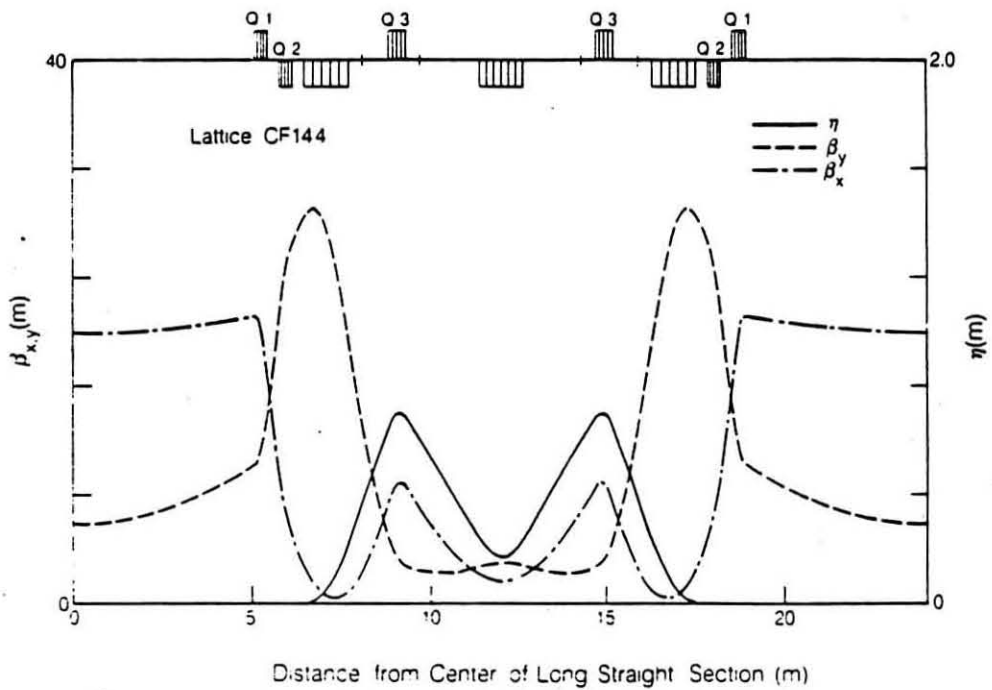
Fig. 2 Dependence of the peak current,  $\bar{i}$ , equilibrium emittance,  $\epsilon_x$ , and some FEL parameters ( $\rho$ ,  $l_e$ ) on the momentum spread,  $\sigma_p$ . Degradation of performance ( $\rho_{\text{eff}}$ ,  $l_{\text{eff}}$ ) with increasing momentum spread is apparent. A Lorentzian momentum distribution was assumed in the calculation of the degradation [see Eqn. (2.17)].

XBL 854-10173



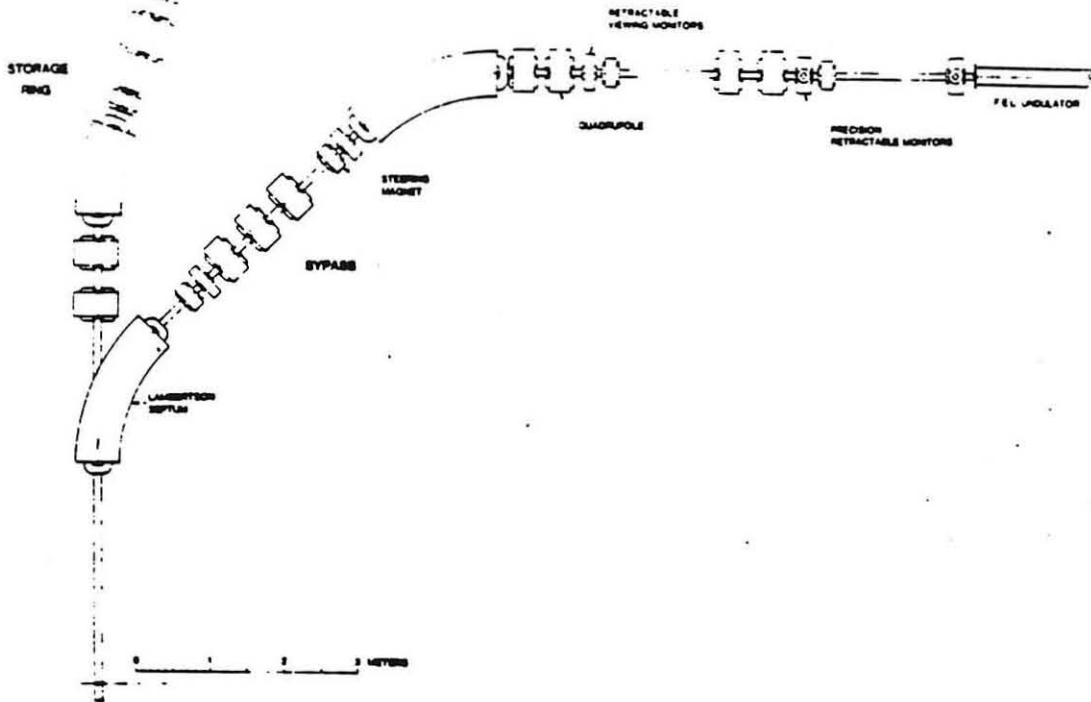
XBL 854-2286

Fig. 3 Schematic layout of ring CF144 and bypass.



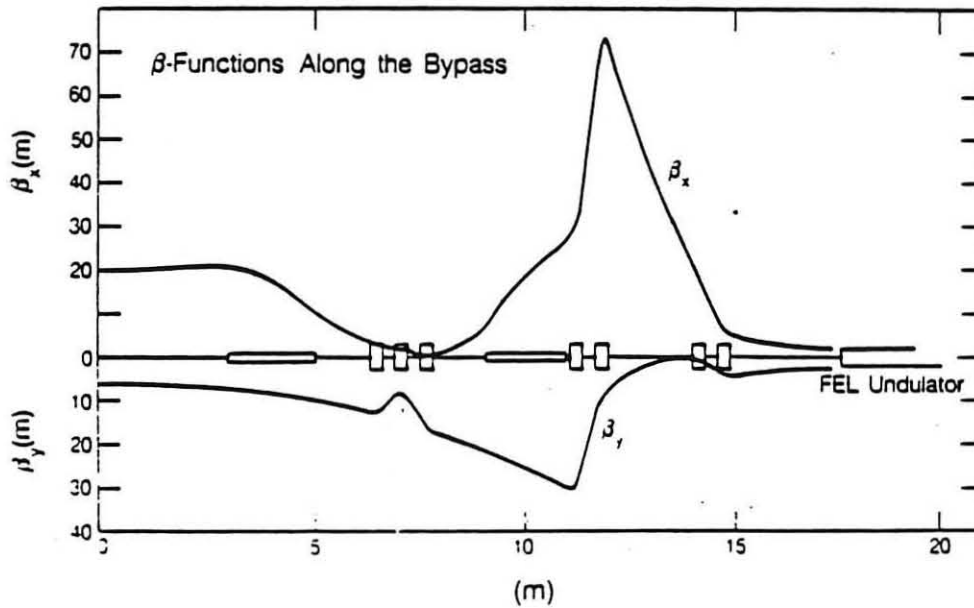
XBL 854-2286

Fig. 4 Lattice structure and functions in one period of lattice CF144. The pattern repeats six times around the ring.



XBL 854-1996

Fig. 5 Layout of the transfer line to the FEL undulator.



XBL 854-10163

Fig. 6 Evolution of the  $\beta$ -function in the bypass.